Bulletin of the Seismological Society of America, Vol. 93, No. 4, pp. 1670–1678, August 2003

Use of Active Fault Data versus Seismicity Data in the Evaluation of Seismic Hazard in the Granada Basin (Southern Spain)

by José A. Peláez Montilla, Carlos Sanz de Galdeano, and Carlos López Casado

Abstract In this article we evaluate the seismic hazard in the Granada Basin (southern Spain), using for the first time the slip rate of known active faults. Our study, as an attempt to compute seismic hazard using active fault data in low to moderate seismicity regions, relies on a complete database of these faults containing information relevant to their seismic potential. We obtain peak ground acceleration values above 0.4*g* for a return period of 475 years. This result is compared with previous evaluations carried out on the basis of the historical seismicity of the area and the application of the well-known theorem of total probability. In these cases, maximum values of 0.2*g* are obtained. We explain the discrepancies found between the slip rate–derived and seismicity-derived estimates of seismic hazard as owing to the different strikes of the faults in relation to the directions of the main stresses affecting the Granada Basin, in the context of the Betic Cordilleras, some of them with evidence of aseismic slip.

Introduction

The Granada Basin is located in the central sector of the Betic Cordillera (southern Spain). It is a basin filled with upper Miocene to Quaternary sediments, and it became individualized in the Pliocene. There are several clearly active faults in this basin, which on the whole facilitate uplifting of the eastern blocks and relative sinking of the western blocks. This phenomenon is found throughout the cordillera but is exceptionally noticeable in the Granada Basin, in particular in its eastern sector.

This may be the most seismically active zone in all the Iberian Peninsula, and in it have occurred some large earthquakes throughout history, such as the 1884 Andalusian earthquake (I_{MM} = X), and the last important instrumental earthquake in Spain, which took place in Albolote on 19 April 1956, with magnitude m_b 5.0 and a macroseismic intensity of VIII. For this reason, different evaluations of seismic hazard have been made, all based on the seismicity of the region, using both parametric and nonparametric (nonzoning) probabilistic methods.

Naturally, with such methodology the results contain uncertainties that are both random (aleatory) and knowledge based (epistemic). The latter are due to data errors in the earthquake parameters, in the catalog, in the parameters calculated from those data (i.e., magnitude, location, and Gutenberg–Richter *a, b*, and m_{max} values) and the relative lack of knowledge about the attenuation relationships governing each zone. In an attempt to reduce this uncertainty, we have used for the first time a recent database of active faults in the region (Peláez *et al.*, 2001; Sanz de Galdeano *et al.*, 2003) to provide a new earthquake source model for evaluating the seismic hazard of the region. The seismicity parameters are derived from the fault data following the Joyner and Fumal (1985) (J&F) methodology. The results are then compared with previous evaluations of seismic hazard obtained on the basis of seismicity, and the resulting discrepancies are discussed in light of our knowledge on the geodynamics of the region.

Seismic Hazard using Fault-Slip Rates

As already stated, the methodology used for calculation of seismic hazard is that proposed by J&F, which uses the fault slip rates to characterize seismic potential and evaluate seismic hazard. This evaluation excludes the hazard caused by the background seismicity of the region. This is adequate for zones where the seismicity characteristics prevent the establishing of magnitude recurrence models for the known active faults, which is the case in the Granada Basin, where there is a complete lack of palaeoseismic data, making it impossible to establish magnitudes or palaeoseismic recurrence periods for specific faults. Therefore, we have not been able to include a characteristic earthquake model by way of, for example, the method of Wesnousky *et al.* (1983). Besides, the historical seismicity of the region is disperse (Fig. 1), and it is difficult to associate earthquakes with active faults observed on the surface. This means that we cannot establish magnitude recurrence models for specific faults from historical seismicity data. If recurrence modelling were

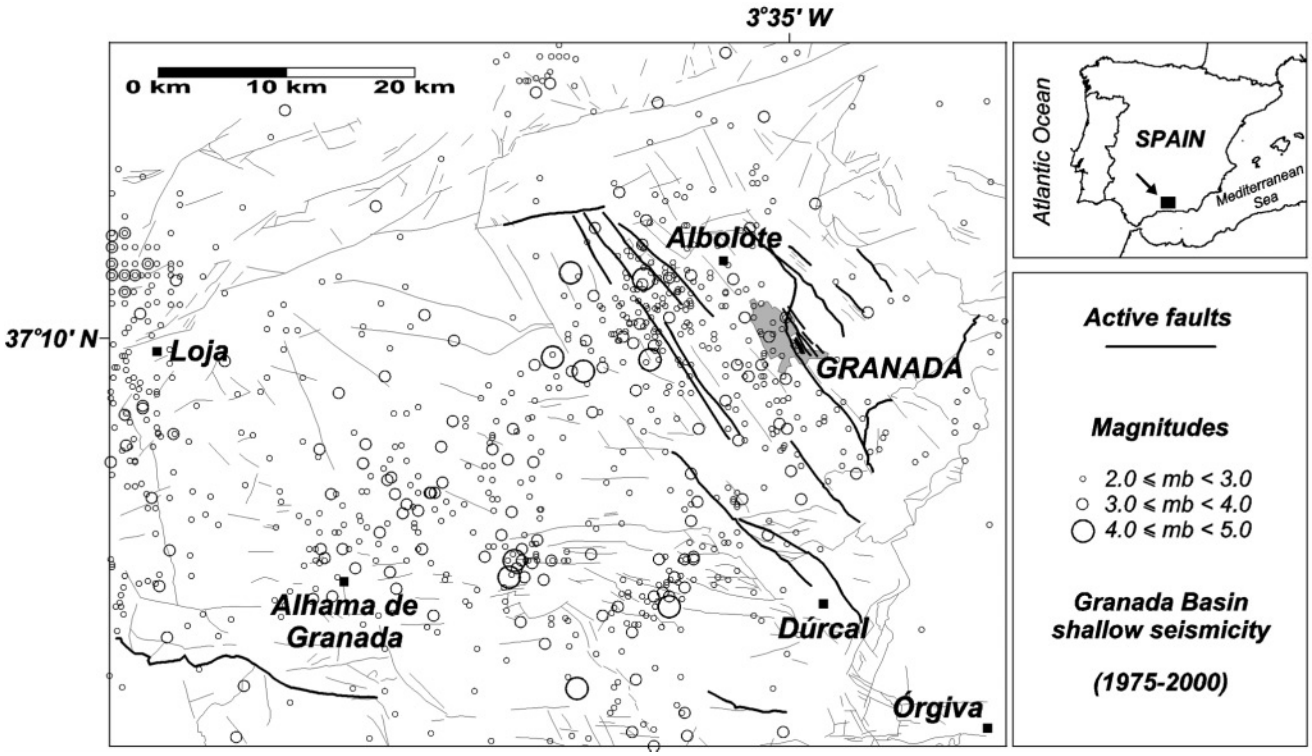

Figure 1. Map showing epicenters and active faults in the Granada Basin and its surrounding area.

possible, we could also consider using methodologies such as those proposed by Cornell (1968), Bender (1984), or Bender and Perkins (1987) to compare with our results, identifying each fault with a seismic source and with a specific magnitude recurrence model.

One of the most significant advantages offered by the J&F methodology is that we do not need to impose a value for the *b* parameter of the fault, as is necessary in other methods (Anderson and Luco, 1983; Wesnousky *et al.*, 1983; Youngs and Coppersmith, 1985). Moreover, using J&F, the result is practically independent of the recurrence relationship of the fault. However, it is not correct to use *b*-values from the region surrounding the fault to characterize it, as has been pointed out in several papers (e.g., Hofmann, 1996), and it is difficult to have the necessary number of earthquakes associated with a fault to be able to assign it its own *b*-value. In our area, the Granada Basin, this is not possible at the moment.

The set of active faults used in this study (Fig. 1), as well as the slip rates, are those shown in Peláez *et al.* (2001) and Sanz de Galdeano *et al.* (2003). Table 1 gives the information necessary for each of these faults. The slip rate data are not as good as we would have wished, in the sense that they were calculated from the vertical displacements observed at several reference levels with an age range of 0.4–10 Ma. We have only used the vertical displacement, which implies that we underestimate the slip rate, and we have carried out a conservative estimate of the age of the reference levels. The errors associated with the estimates of the slip rate are believed to be in most cases less than 10%–15%; this is the estimated error in the evaluation of the age of the used reference levels. Finally, although there is no doubt that these faults are active, we cannot be completely sure that our computed mean rates are still maintained today.

When calculating the seismic hazard caused by a particular fault, the method is as follows. The median value of peak ground acceleration (PGA) is computed for a given return period T as the acceleration value generated by an earthquake (reference earthquake) with a seismic moment equal to

$$M_{0\text{ref}} \cong \frac{\mu}{\alpha}\left(\frac{T}{2}\,v\right)^2 w. \tag{1}$$

Using the Hanks and Kanamori (1979) relationship, this event will have a moment magnitude of

$$M_{\text{Wref}} = \frac{2}{3}\log M_{0\text{ref}} - 10.7. \tag{2}$$

In equation (1), μ is the rigidity modulus, T the return period (the reciprocal of the annual mean rate of occurrence), ν the mean slip rate of the fault, w the total width of the fault capable of causing earthquakes, and α an empirical param-

Table 1
Active Faults Included in This Study

Fault Name, Geometry*	l (km)	d (km)	δ	$\nu^{\dagger}$ (mm/yr)	$T^{\ddagger}$ to 6.0 M_W (yr)	$M_{W\,max}$,[§] σ
North of Sierra Tejeda, $sl - n$	23.1	10	60°–90°	0.13	1300	6.9, 0.3
Granada, n	16.8	10	60°	0.38	510	6.6, 0.2
Padul, n	15.2	5	50°–60°	0.35	1200	6.6, 0.2
Santa Fe, n	13.0	10	[60°]	[0.20]	[1200]	6.5, 0.2
Padul–Dúrcal, n	13.0	5	40°–60°	0.35	1300	6.5, 0.2
Atarfe, n	10.3	10	60°	0.15	2100	6.5, 0.2
El Fargue–Jun, n	11.7	10	60°	0.35	790	6.4, 0.2
Belicena–Alhendín, n	10.4	5	60°	[0.20]	[3100]	[6.4, 0.2]
Albuñuelas, n	9.8	5	40°–60°	0.14	4200	6.4, 0.2
Pinos Puente, n	9.4	10	60°	0.40	860	6.3, 0.2
Dílar, n	8.3	10	60°	0.33	1200	6.3, 0.2
Alitaje, n	6.4	5	40°–60°	0.10	9000	6.3, 0.2
Obéilar–Pinos Puente, $n - sl$	7.9	10	60°–90°	0.50	910	6.2, 0.2
Pedro Ruiz, n	5.9	5	40°–60°	0.10	9700	6.2, 0.2
Huenes, $sl - n$	5.0	10	60°–70°	0.25	2800	6.0, 0.2

These faults have a length equal or greater than 5 km and are ordered according to the estimated value for the maximum magnitude that they can generate (taken from Peláez *et al.* [2001] and Sanz de Galdeano *et al.* [2002]); l is the total length, d is the depth, δ is the dip, ν is the slip rate, T is the return period of magnitude 6.0 M_W, and M_{Wmax} is the maximum moment magnitude that they can generate. Parameters listed in brackets are approximate.

*Geometry: *sl*, strike slip; *n*, normal. The first typology is dominant.

[†]Calculated from the vertical displacement.

[‡]Using the relationship $T = D/\nu$, where D is the average coseismic slip and ν is the slip rate (WGNCEP, 1996).

[§]Using the relationship $M_W = M_W(l, \nu)$ of Anderson *et al.* (1996).

eter relating the length of rupture and the displacement observed in the fault.

This methodology replaces the real earthquake sequence by a fictitious sequence of two earthquakes in a return period T. The PGA generated by one of them (reference earthquake) is, evidently, the median ground-motion value. This method can be applied in such a simple form only when the so-called reference earthquake is not greater than the maximum magnitude the fault can generate. This is the case for all the faults we have considered in our analysis.

The value used for the parameter μ is the typical 3×10^{11} dyne cm^2. Seismic hazard will be calculated in terms of the PGA with a 10% probability of being exceeded in 50 years, that is, the PGA expected with a return period T of 475 years, according to the Poisson model of earthquake occurrence. Table 1 shows the values used for ν, with the conditioning factors mentioned earlier. Additionally, we also consider that the fault is capable of causing earthquakes throughout its depth, and so w is calculated directly using the estimated depth and mean dip of the fault.

Parameter α requires a rather more detailed discussion. In this approximate method, α is defined through the relation

$$u = \alpha \cdot l, \tag{3}$$

where l is the length of rupture and u the displacement observed at the surface (vertically for normal or reverse faults and horizontally for strike-slip faults). We should be able to obtain this information empirically for the area being considered by using the data collected from previous earthquakes. However, the scarcity of data, not only in this zone, but in others of equal or similar characteristics, makes this approach very difficult. The lack of sufficient data on rupture length and displacement is due to the low values of magnitude expected for the reference earthquakes. For example, the maximum value is M_W 5.7 for the Obéilar–Pinos Puente fault.

We have used the few data for faults of these characteristics appearing in the comprehensive study by Wells and Coppersmith (1994). There are only seven earthquakes with reliable data on rupture length and fault displacement for normal faults with rupture lengths less than 20 km, faults similar to those in the Granada Basin. These earthquakes took place at the Fort Sage Mountains (California) on 14 December 1950, Rainbow Mountain (Nevada) on 7 June 1954, Oroville (California) on 1 August 1975, Thessaloniki (Greece) on 20 June 1978, Cuzco (Peru) on 5 April 1986, Kalamat (Greece) on 13 September 1986, and Eureka Valley (California) on 17 May 1993. All of these events had magnitudes between 4.6 and M_S 6.4.

Figure 2 shows the data fit by a straight line passing through the origin with a slope $\alpha = 1.4 \times 10^{-5}$. The correlation coefficient (r^2) is 0.92. Our value for α does not differ appreciably from the 1.1×10^{-5} calculated and used for strike-slip faults in California in the original study by J&F, using information provided by only four earthquakes.

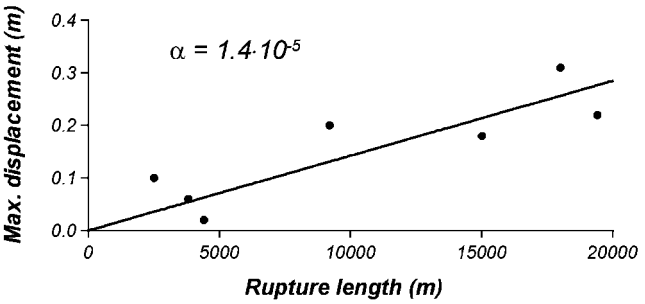

Figure 2. Maximum displacement versus rupture length obtained from the seven chosen earthquakes taken from Wells and Coppersmith (1994).

We use our determined value to calculate the reference earthquake for all the active faults. In Table 1, it can be seen how the strike-slip component dominates over the normal one in two of these faults (north of Sierra Tejeda and Huenes faults). However, the rate data available refer only to vertical displacement. This implies that the seismic hazard assumes that all the faults behave like normal faults.

Once we have calculated the reference earthquake for a particular fault, we can compute the ground motion at some distance from the fault by means of a specific attenuation relationship. The study area has an attenuation coefficient of 0.0070 km^{-1} (López Casado *et al.*, 2000a), which is the same value as, for example, that of Ambraseys (1985) for the northwest European earthquakes. The attenuation relationship we have used is that proposed by López Casado *et al.* (2000a) for this value of the attenuation coefficient. Since this is a relationship established for intensities, we have transformed magnitudes into intensities using the empirical relation derived for the zone by López Casado *et al.* (2000b) and intensities into accelerations using the Murphy and O'Brien (1977) relation. These relations are the most appropriate for the region (Peláez and López Casado, 2002; Peláez *et al.*, 2002). The relation of Murphy and O'Brien (1977) is close to those of Chiaruttini and Siro (1981) and Margotini *et al.* (1987), obtained using data from Italian regions tectonically similar to the Granada Basin. As we are dealing with faults, we have used the Joyner–Boore distance as an independent variable in the attenuation relationship.

The J&F methodology does not explicitly consider the uncertainty of the attenuation relationship or of the parameters used in the calculation. This uncertainty could be included in the study by means of simulations or the logical tree method, for example. This is beyond the scope of our study, although the importance of the uncertainty that our parameters introduce in the hazard assessment is somehow considered when we carry out the sensitivity analysis.

Figure 3 shows the result obtained. Two hazard lobes can be seen at the northeastern and southwestern ends of the basin, coinciding, obviously, with the mapped groups of active faults. At the northeastern end, where almost all of the active faults are located, acceleration values above 0.4*g* are found. At the southwestern end, where only one active fault has been defined, these values exceed 0.2*g*. Table 2 gives acceleration values for the locations shown in Figures 1 and 3, namely Granada, Dúrcal, and Albolote in the eastern part of the Granada Basin; Alhama de Granada to the southwest; and Loja and Órgiva in the vicinity of, but no longer in, the basin itself.

Sensitivity Analysis

Any analysis of seismic hazard can be greatly improved by including a sensitivity analysis (SSHAC, 1997). We can thus investigate the role played in the final result by individual variations of the different analytical parameters. There are no common criteria for expressing the result of a sensitivity analysis or for the sensitivity calculation itself, which depends to some extent on the chosen hazard calculation method. In this study, and given that simple mathematical relations are used to calculate the reference magnitude, we obtain the sensitivity by a simple mathematical expression.

We can establish a generic definition of the sensitivity (S_{x_i}) of a function y due to a particular variable x_i as the relative variation experienced by the function due to a relative unit variation of the variable. We express this mathematically as

$$S_{x_i} = \frac{\Delta y/y}{\Delta x_i/x_i}. \tag{4}$$

In the limit of small variations, we have

$$S_{x_i} = \frac{x_i}{y}\frac{\partial y}{\partial x_i}. \tag{5}$$

To evaluate the sensitivity using this expression, and apply it to the expression resulting from replacing equation (1) into equation (2), we can write

$$S_w = -S_\alpha = \frac{1}{2}S_\nu \cong \frac{1.5}{M_{W\text{ref}}}. \tag{6}$$

We can conclude that the calculation of the reference magnitude is twice as sensitive to ν as it is to w or α. For example, a 100% increase in the values of w or α would affect the magnitude reference value by 0.2 units. The increase would be positive for w and negative for α. On the other hand, a 100% increase in the value of ν would affect the magnitude reference value of the fault by 0.4 units for a given return period.

We recomputed the hazard at the six places given in Table 1. We decreased the values of w and ν separately for all the faults in the basin to a half, a third, and a quarter of their original value (decreasing w by a given percentage is equivalent to increasing α by the same percentage). The re-

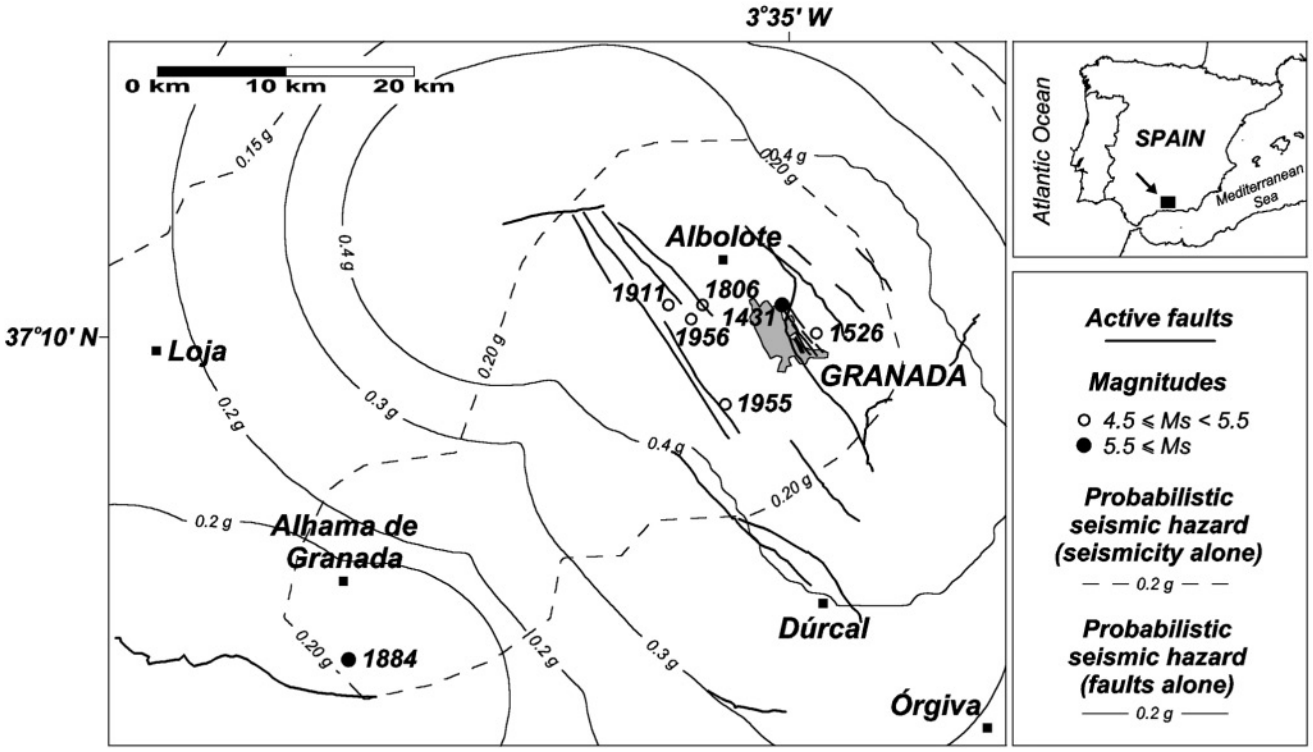

Figure 3. Probabilistic seismic hazard based on seismicity data alone and active fault data alone, in both cases for a return period of 475 years (10% probability of exceedance in 50 years). The most energetic earthquakes in the area are shown with their year of occurrence.

Table 2
Median PGA Values for a Return Period of 475 Years Obtained at the Six Chosen Cities

City	PGA (*g*)		
	Joyner and Fumal (1985)	Peláez (2000) Results	NCSE-94 (1995) Results*
Albolote	0.44	0.22	0.23
Granada	0.41	0.22	0.24
Dúrcal	0.40	0.18	0.22
Órgiva	0.26	0.16	0.17
Alhama de Granada	0.23	0.21	0.24
Loja	0.18	0.16	0.17

*Mean PGA values for a return period of 500 years.

sults obtained are shown graphically in Figure 4, where we can clearly see how decreasing ν to half of its original value is equivalent to decreasing w to a quarter of its original value (or increasing α fourfold). The significance of these results is discussed later.

Comparison with Previous Probabilistic Studies based on Seismicity Data

We want to compare the seismic hazard obtained with the J&F methodology with the results computed from historical seismicity alone. To do so, we provide the hazard

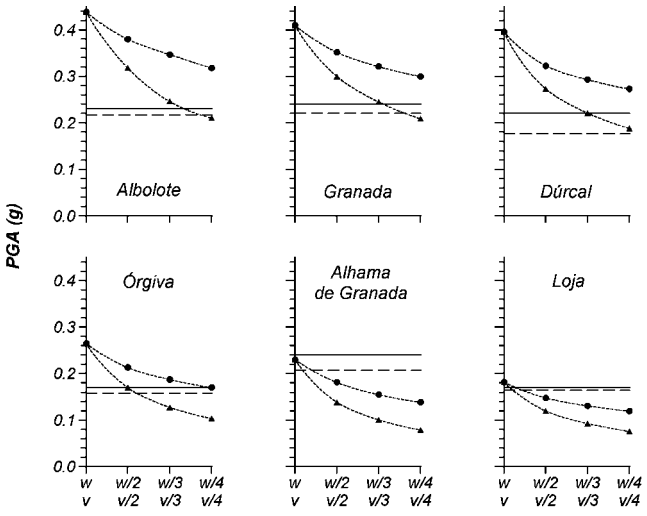

Figure 4. Sensitivity analysis results: PGA values for the for the selected cities. The median peak ground horizontal acceleration for a return period of 475 years, obtained through the J&F methodology, is shown. The calculation has been conducted using decreasing values of the depth (●) and slip rate (▲) for all faults. The values used are one-half, one-third, and one-fourth of the original ones. The horizontal continuous line indicates the hazard reported in NCSE-94 (1995), while the horizontal dashed line is the one obtained in the works of Peláez (2000) and Peláez and López Casado (2002).

results obtained using historical seismicity, for a 475-year return period, by Peláez (2000), Peláez and López Casado (2002), and Peláez *et al.* (2002). Their calculations included earthquakes occurring in the vicinity of the Iberian Peninsula since the year 1300 with a macroseismic magnitude above 5.5 M_S. The specific acceleration values for the locations of interest are shown in Table 2. Figure 3 shows the results of Peláez and López Casado (2002), which can be compared with those obtained by the J&F methodology. The whole zone that shows PGA values above $0.1g$, exceeding $0.2g$ in the southwestern and northeastern zones of the Granada Basin, coincides, to some extent, with the maximum hazard lobes resulting from the J&F methodology. As expected, these two lobes also coincide with the areas where the largest earthquakes have occurred. We are referring to the Arenas del Rey earthquake (in the vicinity of Alhama de Granada) on 25 December 1884 (I_{MM} = X), in the southwestern part of the basin, and the earthquakes of Atarfe on 24 April 1431 (I_{MM} = IX), Granada on 4 July 1526 (I_{MM} = VIII), Santa Fe on 27 October 1806 and on 31 May 1911 (both with I_{MM} = VIII), La Zubia on 4 June 1955 (I_{MM} = VII and magnitude m_{bLg} 5.1), and Albolote on 19 April 1956 (I_{MM} = VIII and magnitude m_{bLg} 5.0). All of these events occurred in the northeastern part of the Granada Basin. Figure 3 shows the epicenters of these earthquakes. The seismicity data used are those of the recent edition of the seismic catalog of Mezcua and Martínez Solares (1983).

Table 2 also presents the values of seismic hazard as defined by the Spanish regulations for seismic-resistent building (NCSE-94, 1995), mandatory for all projects and buildings undertaken in Spain. In this case, the values indicated were obtained through a parametric method.

In the westernmost part of the basin, for all the cities considered, with the exceptions of Loja and Alhama de Granada, the J&F methodology gives higher hazard values than those calculated from seismicity data (Table 2). The median acceleration values found in the eastern locations of the basin (Granada, Albolote, and Dúrcal), for the return period considered, were approximately twice those calculated using seismicity data alone. However, we only considered hazard caused by active faults, excluding the hazard due to the disperse seismicity of the zone. Also, if we had used recurrence relationships for the faults, for example, the Gutenberg–Richter relation, we would have obtained seismic hazard values greater than those derived with the J&F methodology or with the characteristic earthquake model, as pointed out by Frankel *et al.* (1996).

Another question is the fact that the earthquake catalog may overestimate certain maximum intensities of historic earthquakes. Thus, for example, Espinar *et al.* (1994) considered that the Atarfe earthquake of 1431 (I_{MM} = IX) actually consisted of two earthquakes, one located around 100 km from the basin and another one in the vicinity of Granada. The latter did not reach an intensity of IX according to the damage reported. In the cases of other large earthquakes, the overestimation can be deduced from the attenuation relationships inferred from isoseismal maps. Attenuation coefficients of up to 0.083 km^{-1} are reported (López Casado *et al.*, 2000a), almost 10 times higher than those found for other large earthquakes in the Iberian Peninsula, without a physical cause. This indicates that the epicentral intensity values given are overestimated, explaning the fast intensity attenuation. We believe that the accelerations obtained in the seismic hazard evaluations based on seismicity should be even somewhat lower.

On the other hand, it would be hard to get results by using the J&F methodology similar to those obtained from seismicity data alone, using plausible values for the fault depth or α, at the eastern locations in the basin (Fig. 4). This requires present (Holocene) fault slip rates to be only between a half and a third of those calculated on the basis of the vertical displacement. However, there are no reasons to think so.

Summary and Conclusions

We calculated the seismic hazard in the Granada Basin on the basis of the slip rates of known active faults, using the J&F methodology. Comparison with the hazard calculated using parametric (NCSE-94, 1995) or mixed methods using spatially smoothed seismicity data (Peláez and López Casado, 2002; Peláez *et al.*, 2002) gives significantly different results. Probabilistic seismic hazard analysis based on seismicity data alone underestimate seismic hazard in areas of active faults (i.e., Stirling and Wesnousky, 1998; Chang and Smith, 2002). Specifically, we obtained PGA values for a return period of 475 years that are about twice as high as those resulting from seismicity alone. This happens in the area where most of the mapped active faults are located. These hazard values could certainly be reached if the slip observed in each fault occurred as established by the J&F methodology.

The known fault parameters necessary for calculation of the reference magnitude—depth and slip rate—seem to be basically correct. There is nothing to suggest that slip rates during the Holocene are different from the ones used here. Also, and in view of the sensitivity study, very different and scarcely plausible α values would be required to have a significant effect on the result.

We believe that PGA values obtained using the slip rate of known active faults are not to be expected in our area of study. First, the b parameter of the Gutenberg–Richter relationship has a value of 1.1 throughout the geological domain of the Betic Cordillera (López Casado *et al.*, 1995), including the Granada Basin. If we restrict the seismicity data to the last 50 years, the b-value in this domain rises to 1.5 (Buforn and Bezzeghoud, 2001). These large values indicate rapid dissipation of stresses in the zone, preventing the accumulation of energy. This statement becomes still more evident if we notice the remarkable microseismicity observed in this region (i.e., Morales *et al.*, 1997; Muñoz *et al.*, 2002).

The microseismicity and *b*-values are due to the fact that the faults striking northwest–southeast facilitate the northeast–southwest extension in the Betic Cordillera, as shown in Figure 5. This cordillera has both an approximately north-northwest–south-southeast horizontal compression and a practically perpendicular extension, which generally causes uplifting of the blocks situated on the eastern parts of the fault blocks and a sinking of the western ones (Muñoz *et al.*, 2002). This extension is, in many cases, its most remarkable feature at present. However, the approximately east–west–striking faults do not assist extension in the same way, and this explains why we do not observe high slip rate values in the southwestern part of the basin. Consequently, high values of seismic hazard are not obtained.

Another problem is that fibrous growths of minerals such as calcite, gypsum, or iron oxides are found on the exposed surfaces of the faults, indicating the strike and direction of block displacement. This feature is not compatible with sudden movements and needs slow and continuous displacements, indicating that part of the movements of the faults corresponds to aseismic creep (e.g., Behr *et al.*, 1990; Deng and Sykes, 1997; Beeler *et al.*, 2001; Dragert *et al.*, 2001). Detailed palaeoseismic studies are required for each fault to determine which part of its total displacement is seismic and which aseismic. New segmentation studies of these faults will also be necessary.

Moreover, most of the active faults in the Granada Basin are parallel and partially arranged en echelon (see Fig. 5). We therefore interpret that the displacements, by creep or by earthquakes, are distributed among the faults, in such a way that the energy cannot be accumulated easily because there are many faults in which it can be dissipated, preventing the concentration of displacements in a single fault.

Last but not least, the high values obtained in the seismic hazard assessment using faults are brought into doubt in view of the nature of our historical seismicity catalog. In some countries catalogs are at the very most complete for the last 100 or 150 years, even for moderate and high magnitudes. However, in southern Europe, and specifically in the Iberian Peninsula, we have complete catalogs for these magnitudes covering the last 700 years (Peláez and López Casado, 2002; Peláez *et al.*, 2002). Indeed, in some regions like the Granada Basin, we are sure that no destructive earthquake (above 0.4*g* or 0.5*g*) is missing from our catalog in the last 1000 years. Evidently, our catalog and the return period calculated for some of these faults (see Table 1) do not agree.

These are the reasons why we prefer to show the results separately and not added together. We are fully confident about the results obtained through seismicity data alone, but we think that those obtained using active fault data alone are still far from being definitive. In fact, no seismic hazard assessment is definitive (Brillinger, 1982).

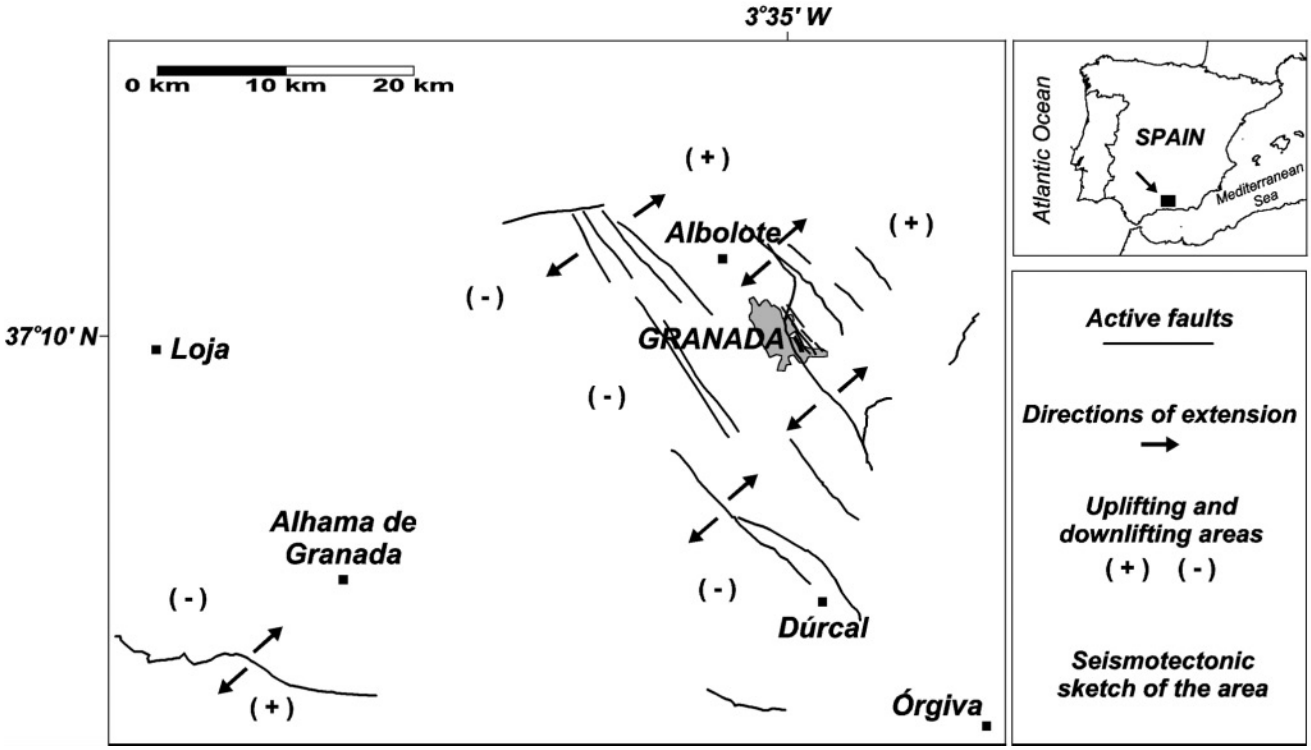

Figure 5. Plot of the directions of extension, uplifting, and downlifting areas (simplified from Sanz de Galdeano and López Garrido, 2000).

Acknowledgments

We thank Dr. Mark Stirling, Dr. Francisco Chávez-García, and an anonymous referee for their reviews and very useful comments and suggestions, which improved the manuscript. This work was supported by the Dirección General de Enseñanza Superior e Investigación Científica (Projects REN2000-0777-C02-01 RIES and PB97-1267-C03-01) and the RNM-0217 Research Group of the Junta de Andalucía.

References

Ambraseys, N. (1985). Intensity–attenuation and magnitude–intensity relationships for northwest European earthquakes, *Earthquake Eng. Struct. Dyn.* **13,** 733–778.

Anderson, J. G., S. G. Wesnousky, and M. W. Stirling (1996). Earthquake size as a function of fault slip rate, *Bull. Seism. Soc. Am.* **86,** 683–690.

Beeler, N. M., D. L. Lockner, and S. H. Hickman (2001). A simple stick-slip and creep-slip model for repeating earthquakes, and its implication for microearthquakes at Parkfield, *Bull. Seism. Soc. Am.* **91,** 1797–1804.

Behr, J., R. Bilham, P. Bodin, R. O. Burford, and R. Bürgmann (1990). Aseismic slip on the San Andreas fault south of Loma-Prieta, *Geophys. Res. Lett.* **17,** 1445–1448.

Bender, B. (1984). Seismic hazard analysis using a finite fault rupture model, *Bull. Seism. Soc. Am.* **74,** 1899–1923.

Bender, B., and D. Perkins (1987). SEISRISK III: a computer program for seismic hazard estimation, *U.S. Geol. Surv. Bull. 1772.*

Brillinger, D. R. (1982). Seismic risk assessment: some statistical aspects, *Earthquake Predict. Res.* **1,** 183–195.

Buforn, E., and M. Bezzeghoud (2001). Seismicity and focal mechanisms of the Ibero-Maghrebian region, in *Workshop on the Geodynamics of the Western Part of Eurasia–Africa Plate Boundary* (*Azores-Tunisia*), San Fernando, Spain, 31 May–2 June 2001.

Chang, W. L., and R. B. Smith (2002). Integrated seismic-hazard analysis of the Wasatch Front, Utah, *Bull. Seism. Soc. Am.* **92,** 1904–1922.

Chiaruttini, C., and L. Siro (1981). The correlation of peak ground horizontal acceleration with magnitude, distance, and seismic intensity for Friuli and Ancona, Italy, and the Alpide Belt, *Bull. Seism. Soc. Am.* **71,** 1993–2009.

Cornell, C. A. (1968). Engineering seismic risk analysis, *Bull. Seism. Soc. Am.* **58,** 1583–1606.

Deng, J. S., and L. R. Sykes (1997). Stress evolution in southern California and triggering of moderate-, small-, and micro-size earthquakes, *J. Geophys. Res.* **102,** 24,411–24,435.

Dragert, H., K. L. Wang, and T. S. James (2001). A silent slip event on the deeper Cascadia subduction interface, *Science* **292,** 1525–1528.

Espinar, M., J. J. Quesada, and J. Morcillo (1994). *Earthquakes in Granada* (*15th and 16th centuries*), *Construction and Seismicity*, Arráez, Almería, Spain (in Spanish).

Frankel, A., Ch. Mueller, T. Barnhard, D. Perkins, E. V. Leyendecker, N. Dickman, S. Hanson, and M. Hopper (1996). National seismic hazard maps, June 1996 documentation, *U.S. Geol. Surv. Open-File Rept. 96-532.*

Hanks, T. C., and H. Kanamori (1979). A moment magnitude scale, *J. Geophys. Res.* **84,** 2348–2350.

Hofmann, R. B. (1996). Individual faults can't produce a Gutenberg–Richter earthquake recurrence, *Eng. Geol.* **43,** 5–9.

Joyner, W. B., and T. E. Fumal (1985). Predictive mapping of earthquake ground motion, in *Evaluating Earthquake Hazards in the Los Angeles Region: An Earth-Science Perspective*, J. I. Ziony (Editor), *U.S. Geol. Surv. Profess. Pap. 1360*, 203–220.

López Casado, C., S. Molina, J. Delgado, and J. A. Peláez (2000a). Attenuation of intensity with epicentral distance in the Iberian Peninsula, *Bull. Seism. Soc. Am.* **90,** 34–47.

López Casado, C., S. Molina, J. J. Giner, and J. Delgado (2000b). Magnitude–intensity relationships in the Ibero–Moghrebian region, *Nat. Hazards* **22,** 269–294.

López Casado, C., C. Sanz de Galdeano, J. Delgado, and M. A. Peinado (1995). The *b* parameter in the Betic Cordillera, Rif, and nearby sectors: relations with the tectonics of the region, *Tectonophysics* **248,** 277–292.

Margottini, C., D. Molin, B. Narcisi, and L. Serva (1987). Intensity vs. acceleration: Italian data, in Proc. of the Workshop on Historical Seismicity of the Central-Eastern Mediterranean Region, C. Margottini and L. Serva (Editors), ENEA-IAEA, Rome.

Mezcua, J., and J. M. Martínez Solares (1983). Seismicity of the Ibero–Maghrebian area, Instituto Geográfico Nacional Report (in Spanish).

Morales, J., I. Serrano, F. Vidal, and F. Torcal (1997). The depth of the earthquake activity in the Central Betics (southern Spain), *Geophys. Res. Lett.* **24,** 3289–3292.

Muñoz, D., A. Cisternas, A. Udías, J. Mezcua, C. Sanz de Galdeano, J. Morales, M. Sánchez-Venero, H. Haessler, J. Ibáñez, E. Buforn, G. Pascual, and L. Rivera (2002). Microseismicity and tectonics in the Granada Basin (Spain), *Tectonophysics* **356,** 233–252.

Murphy, J. R., and L. J. O'Brien (1977). The correlation of peak ground acceleration amplitude with seismic intensity and other physical parameters, *Bull. Seism. Soc. Am.* **67,** 877–915.

Norma de Construcción Sismorresistente Española 1994 (NCSE-94) (1995). Code of earthquake-resistant building: General part and construction, *B.O.E.* 08/02/1995, 3935–3980 (in Spanish).

Peláez, J. A. (2000). Aggregation and deaggregation of expected accelerations in the Iberian Peninsula using background seismicity, *Ph.D. Thesis*, University of Granada, 183 pp (in Spanish).

Peláez, J. A., and C. López Casado (2002). Seismic hazard estimate at the Iberian Peninsula, *Pure Appl. Geophys.* **159,** 2699–2713.

Peláez, J. A., C. López Casado, and J. Henares (2002). Deaggregation in magnitude, distance, and azimuth in the south and west of the Iberian Peninsula, *Bull. Seism. Soc. Am.* **92,** 2177–2185.

Peláez, J. A., C. Sanz de Galdeano, and C. López Casado (2001). Seismic potential of faults in the Granada Basin (Betic cordillera, Spain), *Bull. Geol. Soc. Greece* **34,** 1595–1600.

Sanz de Galdeano, C., and A. C. López Garrido (2000). The Tortonian to Quaternary faults between Granada and the coast: the western limit of the Nevado–Filabride Complex and the lower Alpujarride units, *Rev. Soc. Geol. España* **13,** 519–528 (in Spanish).

Sanz de Galdeano, C., J. A. Peláez, and C. López Casado (2003). Seismic potential of the main active faults in the Granada Basin (southern Spain), *Pure Appl. Geophys.* **160,** 1537–1556.

Senior Seismic Hazard Analysis Committee (SSHAC) (1997). Recommendations for probabilistic seismic hazard analysis: guidance on uncertainty and use of experts, Lawrence Livermore National Laboratory, Report NUREG/CR-6372 and UCRL-ID-1222160, Berkeley, California.

Stirling, M. W., and S. G. Wesnousky (1998). Comparison of recent probabilistic seismic hazard maps for southern California, *Bull. Seism. Soc. Am.* **88,** 855–861.

Wells, D. L., and K. J. Coppersmith (1994). New empirical relationships among magnitude, rupture length, rupture width, rupture area, and surface displacement, *Bull. Seism. Soc. Am.* **84,** 974–1002.

Wesnousky, S. G., C. H. Scholz, K. Shimazaki, and T. Matsuda (1983). Earthquake frequency distribution and the mechanics of faulting, *J. Geophys. Res.* **88,** 9331–9340.

Working Group on Northern California Earthquake Potential (WGNCEP) (1996). Database of potential sources for earthquakes larger than magnitude 6 in northern California, *U.S. Geol. Surv. Open-File Report 96-705.*

Youngs, R. R., and K. J. Coppersmith (1985). Implications of fault slip rates and earthquake recurrence models to probabilistic seismic hazard estimates, *Bull. Seism. Soc. Am.* **75,** 939–964.

Departamento de Física
University of Jaén
C/Virgen de la Cabeza, 2
Escuela Politécnica Superior
23071 Jaén, Spain
(J.A.P.M.)

Instituto Andaluz de Ciencias de la Tierra
CSIC: University of Granada
Avda. Severo Ochoa, s/n
Facultad de Ciencias
18071 Granada, Spain
(C.S.G.)

Departamento de Física Teórica y del Cosmos
University of Granada
Avda. Severo Ochoa, s/n
Facultad de Ciencias
18071 Granada, Spain
(C.L.C.)

Manuscript received 25 April 2002.